Diffusion pollution of neonicotinoid insecticides in wetland ecosystem: Has the cultivation of different crops become the major sources?

Zhikun Liu[a,b], Song Cui [a,b*], Qiang Fu[a,b], Fuxiang Zhang[a,b], Zulin Zhang[c], Rupert Hough[c], Lihui An[d], Yi-Fan Li [a,b], Leiming Zhang[e*]

[a] *International Joint Research Center for Persistent Toxic Substances (IJRC-PTS), School of Water Conservancy and Civil Engineering, Northeast Agricultural University, Harbin, Heilongjiang 150030, China*

[b] *Research Center for Eco-Environment Protection of Songhua River Basin, Northeast Agricultural University, Harbin, Heilongjiang 150030, China*

[c] *The James Hutton Institute, Craigiebuckler, Aberdeen, AB15 8QH, UK*

[d] *State Environmental Protection Key Laboratory of Estuarine and Coastal Research, Chinese Research Academy of Environmental Sciences, Beijing 100012, China*

[e] *Air Quality Research Division, Science and Technology Branch, Environment and Climate Change Canada, Toronto, Ontario M3H 5T4 Canada*

*Corresponding author: Dr. Song Cui Email: cuisong-bq@neau.edu.cn

Dr. Leiming Zhang Email: Leiming.Zhang@ec.gc.ca

WORD COUNT: 5600

5 FIGURES

2 TABLE

Abstract

Extensive application of neonicotinoid insecticides (NNIs) in agricultural production has resulted in widespread contamination of multiple environmental media. To investigate the occurrence and fate of NNIs in the largest marsh distribution area in Northeast China, an integrated ecosystem covering farmlands, rivers, and marshes, referred to as the farmland-river-marsh continuum in this study, was chosen for soil, water, and sediment sampling. Five NNIs were detected, with imidacloprid (IMI), thiamethoxam (THM), and clothianidin (CLO) being the most frequently detected ones in different samples. Concentrations of target NNIs in soil, surface water, and sediment samples were 2.23-136 ng/g dry weight (dw), 3.20-51.7 ng/L, and 1.53-8.40 ng/g dw, respectively. In soil, NNIs were detected more often and at higher concentrations in upland fields, while the concentration of NNIs in the soybean-growing soil (71.5 ng/g dw) was significantly higher than in the rice-growing soil (18.5 ng/g dw) ($p < 0.05$). Total concentration of NNIs in surface water was lower in the Qixing River channel than inside the marsh, while that in sediments showed an opposite trend. Total migration mass of IMI from approximately 157,000 ha of farmland soil by surface runoff was estimated to be 2,636-3,402 kg from the application time to the sampling period. The storage of NNIs in sediments was estimated to range from 45.9-252 ng/cm^2. Risk assessment revealed that 80% and 15% of the surface water samples had NNIs concentrations exceeding the thresholds of long- (35 ng/L) and short-term risks (200

ng/L), respectively, suggesting possible risks posed by NNIs to sensitive aquatic invertebrates.

Keywords: neonicotinoid insecticides, wetland ecosystem, surface runoff, mass inventory, risk assessment.

1. Introduction

Neonicotinoid insecticides (NNIs) are synthetic chemical pesticides similar in structure and action to nicotine and have been often applied in agricultural production worldwide in recent years due to their high efficiency, broad-spectrum, and systemic activity (Morrissey et al., 2015; Mahai et al., 2021). The rapid development of NNIs has eased the tension between the growing human demand for agricultural products and the high incidence of crop pests and diseases. However, the massive use of NNIs also raised widespread global concerns over their environmental effects. For example, NNIs can cause "colony collapse disorder" for bees and seriously reduce the number of pollinators (Cox-Foster et al., 2007). Toxic residues of NNIs have been detected in water bodies, which are likely responsible for the declining populations of aquatic insects (Van Dijk et al., 2013) and insectivorous birds (Hallmann et al., 2014). In addition, there are increasing evidence from *vitro* and in *vivo* experiments demonstrating NNIs' toxicity on hepatic, immune, endocrine, reproductive system, and growth and development of mammals (Chen et al., 2020; Han et al., 2018; Gibbons et al., 2015). Nowadays, the harm to non-target organisms caused by NNIs has led to banning or strict restrictions on their use in many European countries and North America (Liu et al., 2021, 2022; Mahai et al., 2021).

NNIs can accumulate in soil as a result of their widespread and long-term use, and can migrate to aqueous environment through precipitation, runoff, and infiltration due to their high water solubility (Niu et al., 2022; Liu et al., 2021, 2022; Huang et al., 2020).

NNIs have been detected in many rivers and lakes in China, such as the Yangtze River (Chen et al., 2019; Mahai et al., 2019; Wan et al., 2019), Pearl River (Xiong et al., 2019), Songhua River (Liu et al., 2021), Taihu Lake (Zhou et al, 2020), and Dongting Lake (Chen et al., 2019). The levels of NNIs are as high as several thousand ng/L in water bodies and several hundred ng/g in sediments (Niu et al., 2022). These existing studies mostly focused on the pollution status of NNIs in Chinese river systems, while studies on integrated ecosystems are still lacking.

Wetlands are unique ecosystems not only rich in biodiversity, but also regulating the environment (Lu and Wang, 1996; Main et al., 2017). As one of the most dominant wetland types, marsh wetlands play an extremely important role in global ecological balance and security (Keddy, 2010). A large portion of China's fresh-water marsh wetlands is located in Northeast China, among which the Sanjiang Plain is the largest marsh area nationwide (Lu et al., 1996). As most of the marsh wetlands within the Sanjiang Plain have been converted to farmlands, the existing rivers and marsh wetlands are thus surrounded by farmlands, which has substantially increased the hydrological link and material exchange between the river-marsh system and the surrounding agricultural land, and thus created a unique farmland-river-marsh continuum. The Qixing River basin in the Sanjiang Plain is a typical epitome of the farmland-river-marsh continuum. Existing pollution studies for the Qixing River basin mainly focused on heavy metals and water quality (Cui et al., 2020a; Zhang et al., 2020, 2021). A systematic research on the occurrence, spatial distribution, and environmental

behavior of NNIs in water, sediments, and soils in the Qixing River basin is still lacking. To fill this knowledge gap, eight typical NNIs in the farmland-river-marsh continuum of the Qixing River basin were investigated. A major hypothesis of this study was that fluctuations of NNIs concentrations should reflect changes in land use types and hydrology in the farmland-river-marsh continuum. To test this hypothesis, samples in various environmental media, including surface water, sediment, and soil, were collected from the river, marsh, and surrounding farmland for NNIs analysis. The specific goals of this study are to (1) investigate contamination status and spatial distributions of NNIs in a typical farmland-river-marsh continuum; (2) quantify the migration mass of NNIs from the soil to water bodies through surface runoff; (3) estimate the mass of NNIs stored in sediments, and (4) assess the ecological risks of NNIs in the aquatic ecosystem. Results from this study improve our understanding on the occurrence, distribution, and environmental behavior of NNIs and provide much-needed data for risk assessment related to NNIs in the largest marsh area in China.

2. Methodology

2.1 Study area

The Sanjiag Plain, with wetlands all over and rivers running through it, is the largest and most typical freshwater marsh distribution area in China and an important ecological barrier in China and Northeast Asia. The main landforms in this plain are Class I terraces and floodplains with low and flat terrain and a wide range of

concentrated and contiguous wetlands. There are 24 wetland nature reserves above the provincial level in Sanjiang Plain, among which 6 are internationally significant wetlands. As a result of large-scale agricultural reclamation and development, the Sanjiang Plain has become an important commercial grain base in China, but it has also led to the existing rivers and marsh wetlands being surrounded by agricultural land, thus forming a farmland-river-marsh continuum with unique structure and function in the largest marsh distribution area in China. The region is dominated by the continental monsoon climate, with long and cold winters and warm and humid summers. The average annual temperature is approximately 2.4℃, and the average annual precipitation is 551.5 mm. Qixing River basin (131°08′ ~ 132°45′E, 46°10′ ~ 46°54′ N) located in the center of this plain has a basin area of 2,953 km^2, approximately 56% of which is farmland. This river basin has been facing increased threats to its fragile ecosystem from continued agricultural development. Nevertheless, the Qixing River wetland in the basin is a primitive marsh that survived the reclamation of farmland in the 1950s, and it is also one of the most well-preserved, representative, and typical primitive natural freshwater marsh wetlands (https://www.ramsar.org/). The surrounding of the Qixing River wetland and the river by farmland makes it the epitome of the natural landscape of Sanjiang Plain. Meanwhile, the Qixing River wetland is also one of the six internationally significant wetlands in the Sanjiang Plain, and is an important habitat and stopover for many migrating birds, including rare and endangered species.

2.2 Sample collection，processing, and analysis

Samples were collected in the farmland-river-marsh continuum in October 2019 (Fig. 1 and Table S1), including a total of 20 surface water samples, 20 sediment samples, and 22 soil samples. At each sampling site at least 1 L of surface water was collected in brown glass bottles using a portable water collector. All water samples were sent to the laboratory immediately and placed in a 4℃ refrigerator. Surface soil and sediment samples were obtained with a stainless steel sampler, and the overall weight of the sediment and soil samples was no less than 500 g. Sediments and soil samples were quickly wrapped in polyethylene bags, shipped to the laboratory, and placed in a refrigerator at -20°C.

Eight typical NNIs (i.e., imidacloprid (IMI), thiamethoxam (THM), acetamiprid (ACE), dinotefuran (DIN), thiacloprid (THA), nitenpyram (NTP), imidaclothiz (IMIT), and clothianidin (CLO)) were determined, and their relevant properties are shown in Table S2. The surface water and sediment samples were extracted, purified, and analyzed according to the methods established by our previous study (Liu et al., 2021). The same treatment procedure as for the sediment samples was also used for soil samples. Samples after pretreatment were filtered through a 0.22 μm PTFE membrane and then analyzed by AB SCIEX Triple Quad 5500 HPLC-MS/MS (Framingham, MA, USA). The details of the chemicals and reagents, sample pretreatment, and instrumental analysis are provided in the *Supporting Information (SI)*.

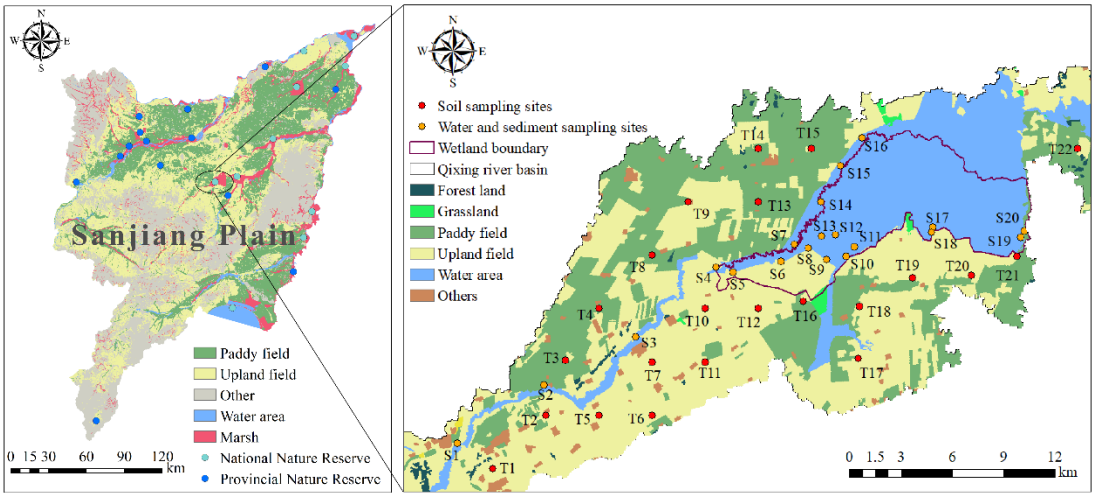

Fig. 1 Sampling sites in the farmland-river-marsh continuum.

2.3 Quality assurance and quality control

Procedural blank, laboratory blank, and matrix spiked samples were used to ensure the sample quality before sample analysis. None of the target NNIs were detected in the blank samples. Meanwhile, three isotope-labeled compounds (CLO-d_3, IMI-d_4, and THM-d_3) were applied to all samples before extraction and used as surrogate standards to check the efficiency of the sample preparation process. The recoveries of the eight target compounds ranged from 86.3-108.9% for water samples and from 79.8-106.5% for sediment and soil samples. The method detection limit (MDL) of target analytes in the sample was calculated from the S/N ratio of 10 (Table S3) (Mahai et al., 2019). If the detected concentration in the sample is lower than the MDL, the value is set to zero.

2.4 Migrated mass by surface runoff

Pesticides in the soil can be transported into the water environment through surface runoff, and the transport amount is calculated as follows (Wang et al., 2019):

$$pst_{surf} = \beta_{pst} \frac{pst_{flow}}{w_{mobile}} \alpha P_i \quad (1)$$

where pst_{surf} is the mass of pesticide transported by surface runoff from a unit area of surface soil (kg/ha); β_{pst} is the pesticide percolation coefficient; pst_{flow} is the amount of pesticide contained in the soil water flux (kg/ha); w_{mobile} is the amount of mobile water (mm); α is the surface runoff coefficient; and P_i is precipitation amount from the time of IMI application to the last rainfall before sample collection (8th October) (mm).

$$pst_{total} = pst_{surf} \cdot Area \quad (2)$$

where pst_{total} is the total mass of pesticide transported by surface runoff (kg); and *Area* is the area under crop cultivation (ha). A detailed derivation process of surface water is presented in the *SI*.

2.5 Mass inventory of NNIs in sediments

The total mass of a chemical in a unit horizontal area of sediments is defined as the mass inventory of the target chemical in sediments (Pan et al., 2022). The mass inventory is calculated as follows:

$$\text{Mass Inventory} = \sum C_i \rho d \quad (3)$$

where C_i is the mean concentration of NNIs in sediments (ng/g dw); ρ is the density of dry sediments (g/cm^3); and d is the depth of sediments (cm). The sediment depth and density were 20 cm and 1.5 g/cm^3, respectively (Pan et al., 2022; Zhang et al., 2018).

2.6 Ecological risk assessment

Ecological risks of a pollutant can be assessed using risk quotients (RQs) according to the Technical Guidance Document on risk assessment (European Commission, 2003):

$$RQs=MEC/PNEC \quad (4)$$

where MEC and PNEC are the measured environmental concentrations of pollutants (ng/L) and the predicted no-effect concentrations (ng/L), respectively. NNIs toxicity data for sensitive aquatic species are presented in Table S4 and PNEC details are in Text S5. The ecological risk level is considered to be low, medium, and high for RQs of <0.1, 0.1-1.0, and >1.0, respectively, according to the RQs classification proposed by Hernando et al. (2006).

2.7 Statistical analysis

Statistical analysis of data was carried out using the IBM SPSS Statistics program (version 26.0). A Fisher least significant difference (LSD) of One-way ANOVA was used to analyze NNIs concentrations among different crop types. For all comparisons, differences were considered significant at $p < 0.05$. The relationship between NNIs and total organic carbon (TOC) in sediments and soil was analyzed using Spearman correlation analysis.

3. Results and discussion

3.1 NNIs contamination in soil, water, and sediments

Concentrations and detection frequencies (DF) of eight NNIs in soil, water, and

sediments in the farmland-river-marsh continuum are summarized in Table 1, with details being listed in Tables S5 to S7. Among the eight examined NNIs, two NNIs (THA and DIN) were not detected in any of the three environmental compartments.

Statistical data of IMI, THM, CLO, ACE, and IMIT in soil from the farmland-river-marsh continuum of the Qixing River basin are displayed in Tables 1 and S5. The majority of soil samples were detected for at least three NNIs (Fig. S1). Total concentration of the five NNIs (Σ_5NNIs) in soil ranged from 2.23-136 ng/g dw, with a mean of 34.8 ng/g dw for 22 soil samples, indicating strong variability (coefficient of variation (Cv=1.3)). The high Cv value of NNIs in soil samples could be attributed to the influence of crop type, specific use mode, and pest species. The mean concentration of individual NNIs in soil decreased in the following order: IMI (29.2 ng/g dw) > THM (3.65 ng/g dw) > CLO (1.88 ng/g dw) > ACE (0.004 ng/g dw) > IMIT (0.001 ng/g dw). The mean IMI concentration in soil was about 8 times higher than that of THM, which is similar to their commercial use ratio (IMI/THM: 7.88) in Heilongjiang Province in 2018, indicating that usage is an important factor influencing the residues of NNIs in soil. The detection frequency was 100% for IMI, THM, and CLO in soil, but only 4.55% for ACE and IMIT. IMI was the predominant compound, accounting for 3% - 95% of Σ_5NNIs in soil (mean: 83.8%), followed by THM (range: 1%-69%; mean: 10.5%) and CLO (range: 1%-32%; mean: 5.41%) (Fig. 2a). Such a pattern is not surprising because IMI has been used the longest and the most among all of the investigated NNIs in China. These results indicate that IMI, THM, and CLO were the main NNIs used in the

farmlands of the study area.

In water samples, five target compounds were detected, namely IMI, THM, CLO, ACE, and NTP (Fig. S1). At least two of the targeted NNIs were detected in all of the 20 water samples, with 65% and 30% of water samples containing three and four NNIs, respectively. As can be seen from Table 1, the detection frequency was high for IMI (100%), CLO (100%), and THM (95%) in the water samples. The concentration of Σ_5NNIs in surface water ranged from 3.20 ng/L to 51.7 ng/L, with a mean of 21.2 ng/L, and showed moderate variability (Cv=0.5). The mean concentration of individual NNIs in water decreased in the following order: THM (9.97 ng/L) ≈ IMI (9.93 ng/L) > CLO (1.26 ng/L) > ACE (0.04 ng/L) > NTP (0.02 ng/L). The residual level of NNIs in water should be influenced by their solubility and usage frequency and amount. It is worth mentioning that although the concentration of IMI in the soil was much higher than that of THM, the higher water solubility, lower log K_{ow}, lower soil adsorption, and longer water photolysis half-life of THM than IMI (Table S2) resulted in the extremely faster leaching of THM from the soil and its more stable presence in the water. As can be seen from Fig. 2b, IMI and THM were the dominant NNIs in wetlands and river water, with their contributions in the range of 29%-89% and 0-64%, respectively. CLO had a high detection frequency, but with low residue levels.

Four NNIs were detected in sediment samples, and the only exception is NTP (Fig. S1). 85% of the sediment samples contained three NNIs and the remaining ones contained four NNIs, meaning a detection frequency of 100% for three NNIs (IMI, THM, and

CLO) and 15% for the fourth one (ACE) (Fig. 2c). Σ_4NNIs ranged from 1.53 to 8.40 ng/g dw, with a mean of 3.66 ng/g dw, and with moderate variability (Cv=0.6). Consistent with the findings for surface water, IMI and THM were dominant NNIs in sediments with a mean concentration of 2.15 ng/g dw and 1.24 ng/g dw, respectively. CLO in sediments maintained at quite low levels, ranging from 0.08-0.73 ng/g dw with a mean of 0.25 ng/g dw. The concentration of ACE in sediments ranged from ND to 0.19 ng/g dw, with a mean concentration of 0.01 ng/g dw. Since ACE concentrations and detection frequencies are lower in soil than sediment, ACE might have entered into sediments in the study area through other pathways, e.g., long-range river transport (Goulson, 2013).

In summary, IMI, THM, and CLO were the most prevalently detected NNIs in the three environmental media in the farmland-river-marsh continuum of the Qixing River basin. It is worth pointing out that the use of IMI, THM, and CLO, especially N-nitroguanidine NNIs, is expected to continue to increase since traditional insecticides, such as organophosphates, pyrethroids, and carbamates, are gradually replaced. Moreover, the concentrations of NNIs in surface soils were generally higher than those in sediments (p<0.05), suggesting that the local farmland soils were an important source of NNIs. These results are consistent with those of the Songhua River, for which IMI, THM, and CLO were detected in all of the surface water and sediment samples (Liu et al., 2021). Thus, the three NNIs might have the same application pattern throughout the Heilongjiang Province of China. Note that, due to the wide range of sources of NNIs,

such as wastewater from sewage treatment plants, agricultural runoff, and urban greening (Ke et al., 2022; Liu et al., 2021; Li et al., 2020), the concentration of NNIs was much higher in the Songhua River (62.3 ng/L) than in the present study. More importantly, strict regulations have been implemented to protect water quality by limiting agricultural activities in the marsh wetland area investigated in this study.

Table 1 Concentrations and detection frequencies (DF) of NNIs in surface water, sediments, and soil collected from the farmland-river-marsh continuum.

Compound	Water (ng/L)			Sediment (ng/g dw)			Soil (ng/g dw)		
	Range	Mean	DF	Range	Mean	DF	Range	Mean	DF
IMI	2.84-25.6	9.93	100%	0.57-6.36	2.15	100%	1.28-133	29.2	100%
THM	ND-24.3	9.97	95%	0.49-2.85	1.24	100%	0.52-29.3	3.65	100%
CLO	0.36-2.47	1.26	100%	0.08-0.73	0.25	100%	0.08-14.8	1.88	100%
ACE	ND-0.28	0.04	20%	ND-0.19	0.01	15%	ND-0.08	0.004	4.55%
NTP	ND-0.19	0.02	10%	ND	ND	0	ND	ND	0
IMIT	ND	ND	0	ND	ND	0	ND-0.01	0.001	4.55%
ΣNNIs	3.20-51.7	21.2	100%	1.53-8.40	3.66	100%	2.23-136	34.8	100%

ND: not detected.

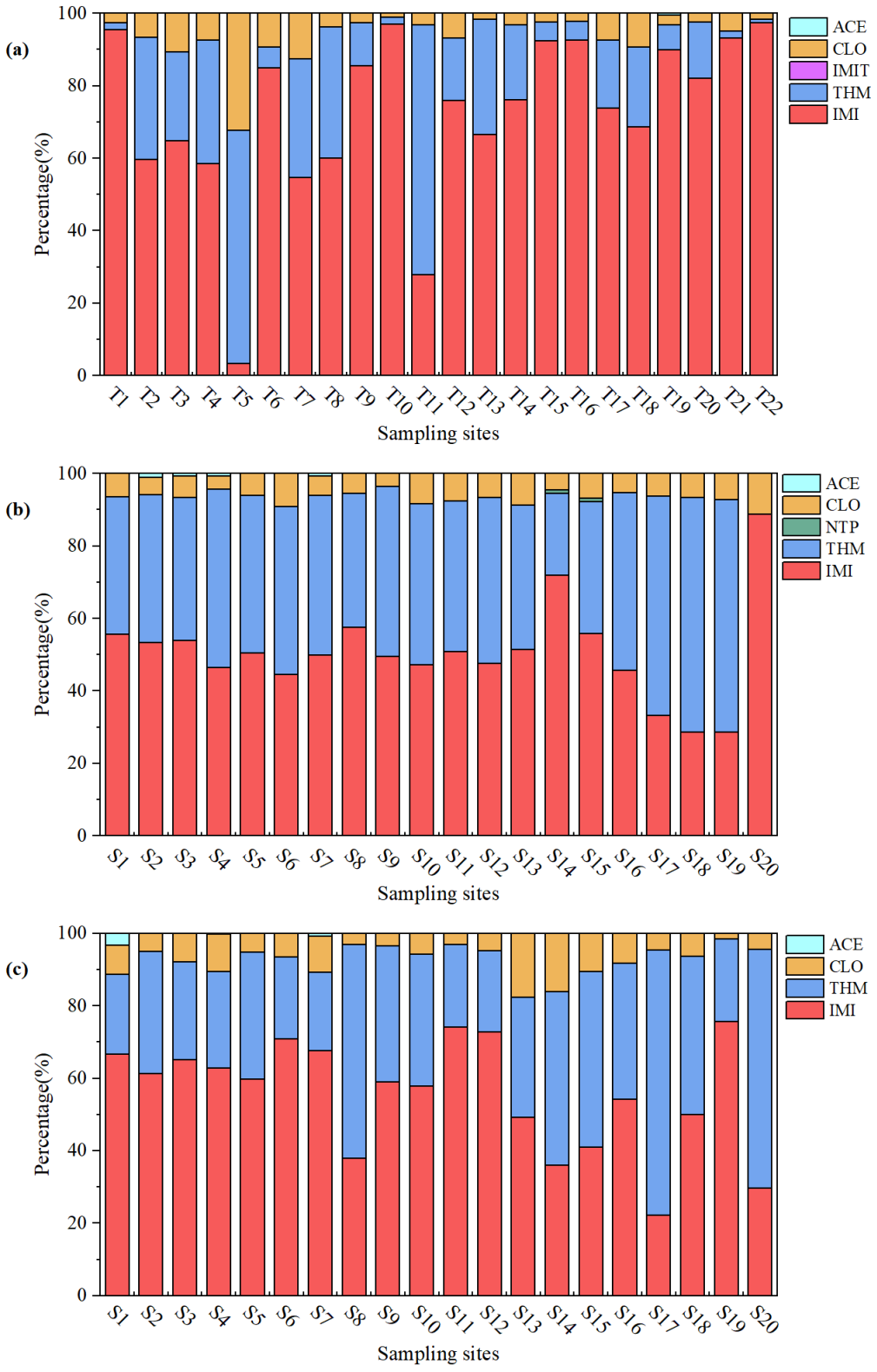

Fig. 2 Composition of NNIs in (a) soil, (b) surface water, and (c) sediment samples collected from the farmland-river-marsh continuum.

3.2 Spatial distribution of NNIs

The concentrations of NNIs in different media of the farmland-river-marsh continuum varied greatly among different sampling sites. Among the soil sampling sites, the highest concentration of Σ_5NNIs (136 ng/g dw) was found at T22, which might be related to crop types grown on the soil since the amount and frequency of NNIs application depended on crop types, as discussed in detail in Section 3.3 below. Of the total NNIs detected in soil, IMI made up the most; therefore, the spatial distributions of Σ_5NNIs were similar to those of IMI (Fig. 3). CLO and THM exhibited similar spatial distribution characteristics, and both had the maximum concentration at T5, indicating their similar application mode in the study area. Note that the registered NNIs products in China mainly include IMI, THM, and ACE, so these three pesticides had high detection rates and concentrations in most earlier studies (Cui et al., 2021; Mahai et al., 2021). However, IMI, THM, and CLO were the top three detected NNIs in the soil samples of this study. The replacement of ACE by CLO was likely due to different crop types planted and different targeted pests in this than earlier studies. CLO covers a broad pest spectrum and has been widely used for seed, soil, and foliar treatment (Jeschke et al., 2011).

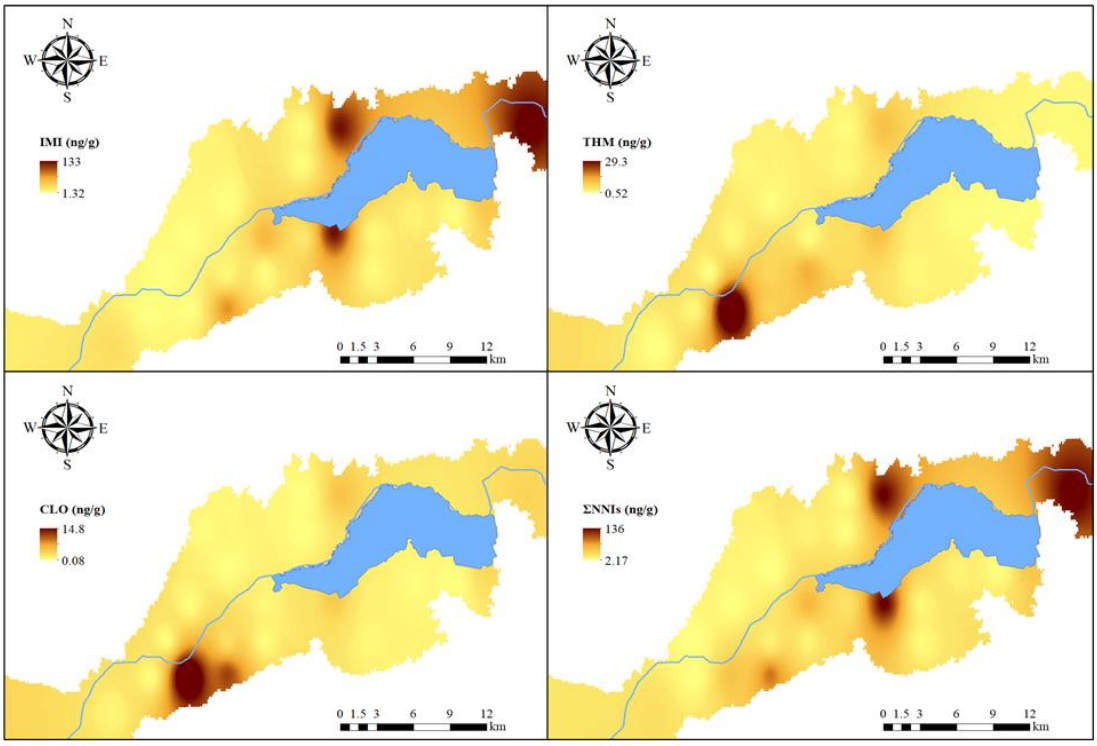

Fig. 3 Spatial distributions of NNIs residues in soil from the farmland-river-marsh continuum. For water sampling, sites S5, S6, S8 to S13, and S17 to S20 are located in the marsh, and sites S1 to S4, S7, and S14 to S16 are located in the Qixing River channel. The mean concentration of NNIs in water was higher inside the marsh (Σ_5NNIs: 22.3 ng/L) than in the Qixing River channel (Σ_5NNIs: 19.6 ng/L), which was likely mostly caused by hydrological factors. The sampling period was in the wet season, with abundant replenishment of water from the upper reaches of the river. Frequent water exchange diluted the NNIs in-stream and transported the NNIs to the marsh. Inside the internal water bodies of the marsh, water flow was slow and water exchange capacity was relatively weak, resulting in relatively weak dilution of NNIs. Among all the sampling sites, S9 was most polluted with NNIs due to the highest IMI and THM concentrations (Fig. 4(a)). This may be due to the high content of NNIs in the farmland in the wetland

experimental zone, which leached NNIs to the surrounding water bodies through runoff after major precipitation events. Topography could be another factor, which controls hydrological elements within the marsh, where NNIs may pool under the influence of hydrodynamic conditions due to the relatively low topography at S9 (from Digital Elevation Model (DEM) data).

In the sediments, the various NNIs presented different distribution characteristics (Fig. 4(b)). For example, the mean concentrations of IMI and CLO were higher in the Qixing River channel than that in the interior of the marsh, while similar mean concentrations of THM were observed (marsh: 1.26 ng/g dw and river: 1.22 ng/g dw). In addition, ACE was only detected in the river sediment sampling sites (S1, S4, and S7), implying that NNIs can migrate through river into the marsh. The distribution pattern of organic contaminants in sediments depends on the physicochemical properties of the contaminants (Bhutto et al., 2021). For example, IMI and CLO have lower solubility, long half-life time, and higher log K_{ow} compared to THM, resulting in their preferential accumulation in sediments due to gravity after entering the water bodies through surface runoff. The total concentration of NNIs in the sediments showed an opposite distribution trend to that in the water body, i.e., with higher concentration in the Qixing River channel (Σ_4NNIs: 4.21 ng/g dw) than the interior of the marsh (Σ_4NNIs: 3.00 ng/g dw). The presence of buffer zone macrophyte communities in the marsh can often "buffer" the impact of human activities (Main et al., 2017). On one hand, macrophytes can change the physical structure and environmental conditions of marsh, which can

slow erosion and filter organic pollutants (Main et al., 2017). On the other hand, macrophytes within the marsh can buffer the effects of pesticides on sediment through sorption, degradation, or root accumulation (Main et al., 2017). In summary, the farmland surrounding the study area is the major source of NNIs, which migrate to the marsh through the river, posing a serious threat to the water environment and water ecological safety of the receiving marsh.

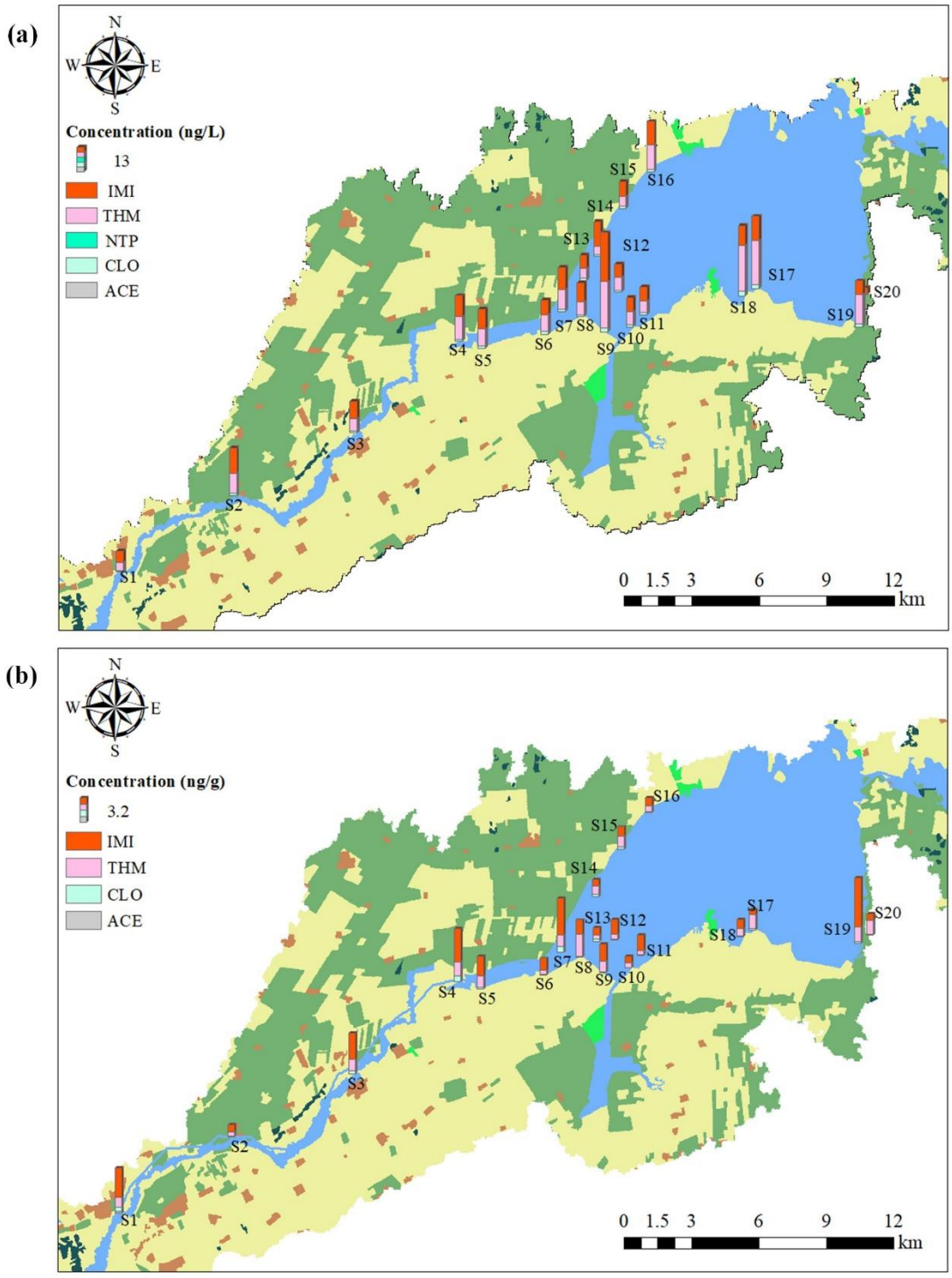

338

339 **Fig. 4** Spatial distributions of NNIs residues in (a) surface water and (b) sediment from the

340 farmland-river-marsh continuum.

341 The relationship between NNIs concentration and sediment/soil organic carbon content

342 was investigated using Spearman correlation analysis (Fig. S2). In sediments, THM (*r*

= 0.48, $p < 0.05$) and the total concentration of four NNIs (Σ_4NNIs, $r = 0.45$, $p < 0.05$) were significantly positively correlated with TOC, while no significant correlation was found for IMI or CLO with TOC ($p > 0.05$). Thus, the residue and distribution of THM and Σ_4NNIs in sediments were likely driven by TOC levels. However, NNIs in the soil were not significantly correlated with TOC ($p > 0.05$), indicating that the residue of NNIs in the soil was hardly affected by the TOC content. The differences in the results between soil and sediment were attributed to their different organic matter properties. The sediments can be originated from the sedimentation of wind-eroded soil particles, run-off soil particles, and suspended sediments from the water bodies. The physicochemical properties of sediments were relatively more stable and less affected by external factors compared to the case of soils. In addition, NNIs in soils were mainly derived from agricultural applications, which were closely related to human agricultural activities and barely affected by TOC in soils. The above results suggest that the distribution of NNIs was influenced by usage patterns, crop types, physicochemical properties of NNIs and environmental media, and runoff conditions, all of which influence the distributions of individual NNIs in different media.

3.3 NNIs residues in soils planted with different crops

To further explore the effects of different crop types on NNIs residues in soil, soil samples were regrouped and analyzed based on crop type grown on the soil. Among the different crop types, soybean-growing soils contained extremely high levels of Σ_5NNIs (71.5 ng/g dw), followed by maize (33.8 ng/g dw), and rice (18.5 ng/g dw) (Fig.

5), indicating that the levels of NNIs residues in soil were significantly correlated with the type of land cultivation.

In soybean-growing soils, IMI was absolutely the dominant contributor to Σ_5NNIs (mean: 92.5%), leaving a small fraction of Σ_5NNIs from THM (mean: 4.90%) and CLO (mean: 2.57%). IMI was also the dominant contributor to Σ_5NNIs in maize- (68.9%) and rice-growing soil (84.2%), although the contributions from THM (maize: 18.4% and rice: 12.6%) and CLO (maize: 12.7% and rice: 3.14%) were also significant. Significant differences in soil IMI concentrations were found between different crops, with the highest one in soybean (66.1 ng/g dw), followed by maize (23.3 ng/g dw) and rice (15.6 ng/g dw) (Fig. 5). Note that with the excessive and frequent use of IMI in the process of rice cultivation, the resistance of pests has also been continuously enhanced, resulting in the restriction of IMI application on rice fields (Bass et al., 2015). In addition, knowing that biological nitrogen fixation occurs during soybean growth, whether this process is responsible for the high residual levels in soybean-growing soils needs further investigation.

In addition, of the three crops mentioned above, maize and soybean are upland crops, while rice is a paddy crop. The concentrations of all of NNIs were higher in upland fields than in paddy fields (Fig. S3). The mean concentrations of IMI, THM, CLO, and Σ_5NNIs in upland fields were 2.74, 2.13, 5.48, and 2.75 times, respectively, of those in paddy fields. Compared with upland field crops, receding water behavior such as artificial drainage and rainfall runoff occurs during the main reproductive period of rice.

Due to the high water solubility of NNIs, receding water from agricultural fields often contains high concentrations of NNIs and can migrate along agricultural ditches to lakes or rivers in the lower part of the region, which was one of the main sources of contamination of water bodies.

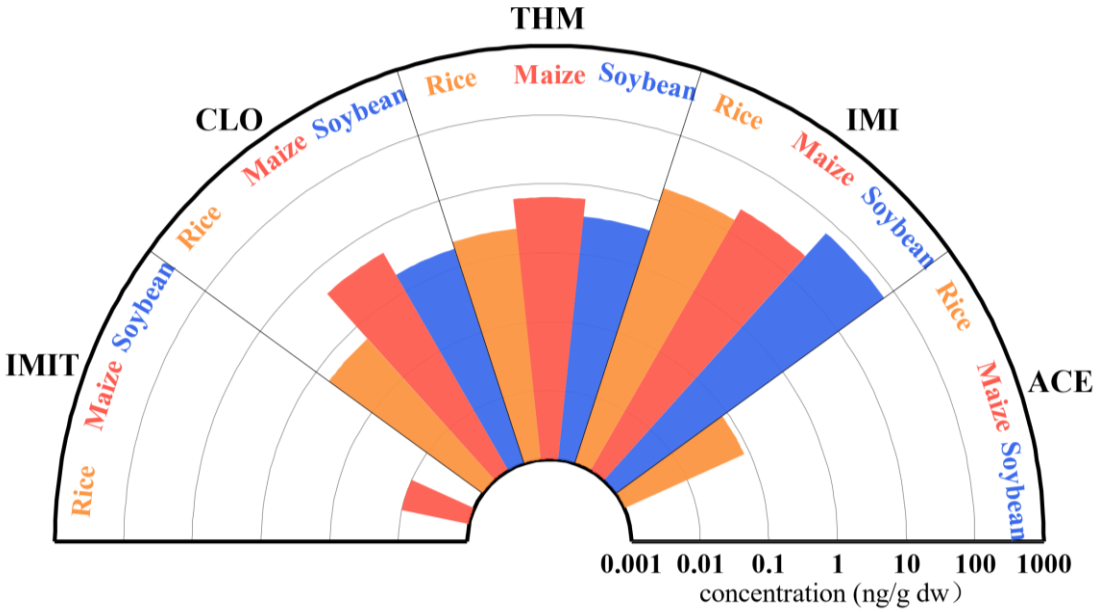

Fig. 5 Mean concentrations (ng/g dw) of different NNIs in various growing soils.

3.4 Migration mass by surface runoff

Once NNIs enter into various environmental media, they are transported and circulated through precipitation scouring and river confluence. Precipitation is the main driving force for the transport of NNIs in soil, accompanied by runoff process that migrate NNIs to river, which in turn pool NNIs in marsh. Considering that IMI is the dominant NNIs used in the study area, we estimated the transport amount of IMI through surface runoff based on precipitation amount, maximum usage, and planted area using Eq. (1). Monte Carlo simulation is often used for uncertainty analysis, and this method is run here by

100,000 iterations (Tang et al., 2020). Results of the sensitivity grade correlation coefficient are shown in Fig. S4.

Half-life time is one of the main parameters reflecting the residual time of a pollutant in soil; therefore, the migration flux of IMI through surface runoff is influenced by the residual time in soil. The range of the half-life of IMI (104-228 d) based on the Pesticide Properties DataBase (PPDB) reported half-life time values was used to estimate the range of IMI migration mass through surface runoff. The total amount of IMI migration through surface runoff from the time IMI was applied to the last rainfall before sample collection (8th October) was estimated to range from 2,636-3,402 kg from a total crop area of 157,096 ha, of which 2,239-2,924 kg were from maize fields (a total area of 71,820 ha), 313-377 kg from rice fields (40,816 ha), and 83.8-101 kg were from soybean fields (44,460 ha). The above results suggest that maize cultivation is the priority land use that needs to be controlled to prevent IMI loss. The highest migration of IMI through surface runoff from maize planting soil was mainly caused by the large usage of IMI per unit area and the large planting area (Tables S8 and S9). Based on the IMI registration information, it was found that the application method for IMI in maize cultivation was seed coating, while for rice and soybean were mainly sprayed for pest control, and the usage amount was higher in seed coating than spray. Thus, the largest planted area, the highest usage of IMI in seed coating, and the highest IMI migration flux per hectare (pst_{surf}) resulted in the highest IMI mass loss from maize fields. The artificial wetland system in rice fields with soil and water conservation characteristics

resulted in a lower surface runoff coefficient (α) than that of upland fields (Table S9) (Liu et al., 2019). However, rice fields had higher migration mass than did soybean fields due to the 6 times higher usage of IMI per unit area in rice than soybean fields.

It is worth noting that the migration of IMI in rice and soybean soils may have been underestimated in the current study. This is because IMI may be used more than once during the crop growth period affected by pest infestation. In addition, farmers might lack of scientific knowledge when applying pesticides, which could spray more IMI than the recommended maximum values. This inference came from our field visits, expert consultations, and the high residual IMI concentrations in soybean-growing soils.

3.5 Mass inventory of NNIs in sediments

NNIs migrated into the river through surface runoff would partially be transported long distances with the water flow and partially accumulated in the sediments. Based on our previous findings, sediments can act as a source of secondary release (Cui et al., 2020b; Liu et al., 2021, 2022), resulting in NNIs entering into the water bodies and accumulating in the sediments through sedimentation, and then re-entering into the water bodies through diffusion and exchange behavior. Therefore, we evaluated the mass inventory of NNIs in the sediments.

The NNIs in sediments at different sites calculated using Eq. (3) ranged from 45.9-252 ng/cm^2, with a mean of 110 ng/cm^2. The area of the Qixing River basin is about 200 km^2, 85% of which is water area. Using the mean value of 110 ng/cm^2 for the whole Qixing River basin, the total load of NNIs in the sediments was estimated to be 187 kg.

This amount of NNIs in sediments can cause damage to the habitat of benthic organisms and thus pose an ecological risk. Furthermore, this amount is likely an underestimate because only parent compounds were considered, with metabolites being excluded. In particular, the metabolites may be more toxic than the parent compound, and can pose higher threats to aquatic organisms. Note that downward diffusion may result in NNIs penetrating into deeper sediments than the case of the actual discharge (Zhang et al., 2022), which was not assessed in this study. Therefore, a stratification study of the sediments would provide a more complete picture on the contamination status and spatial and temporal distributions of NNIs in the sediments.

3.6 Ecological risk assessment

Table 2 shows RQs of five individual NNIs in the water bodies of the farmland-river-marsh continuum in 2019. RQs of each individual NNIs in the water body were all lower than 0.1, indicating low environmental risks. The results of this study were consistent with those reported for the central Yangtze River (Mahai et al., 2019), but higher risks were reported for the rivers surrounding the Bohai Sea (Naumann et al., 2022). Note that the effective concentration (e.g., no observed effect concentration (NOEC), median lethal or effective concentration ($L(E)C_{50}$)) of freshwater species was higher in the Pesticide Properties Database (PPDB) than other databases, such as the ECOTOX database used by Naumann et al. (2022); thus the PNEC values based on PPDB, as generated in the present study, were higher, which led to lower RQs values. Therefore, when using RQs for risk assessment, the data source would have an

important impact on the results, and should be taken into account in uncertainty analysis. Morrissey et al. (2015) proposed a threshold value of 200 ng/L for avoiding short-term acute and 35.0 ng/L for avoiding long-term chronic on aquatic invertebrates. NNIs in surface water were normalized by relative potency factors, as detailed in our previously reported method (Liu et al., 2021). Using the above thresholds (Fig. S5), 15% and 80% of the surface water samples exceeded the acute and chronic risk thresholds, respectively. Therefore, high environmental risks caused by NNIs to sensitive aquatic invertebrate populations likely exist in the study region, which should be made aware to policy makers for making proper environmental protection policies.

Table 2 Risk quotients for NNIs in the surface water of the farmland-river-marsh continuum.

Compound	Most sensitive species	Effective concentration (mg/L)	Endpoint	AF	PNEC (mg/L)	RQs
IMI	*Daphnia magna* (Daphnia)	1.8	NOEC	10	0.18	2.69E-04
THM	*Oncorhynchus mykiss* (Fish)	20	NOEC	50	0.40	2.63E-05
CLO	*Daphnia magna* (Daphnia)	0.12	NOEC	50	2.40E-03	5.25E-04
ACE	*Daphnia magna* (Daphnia)	5	NOEC	50	0.10	1.86E-06
NTP	*Oncorhynchus mykiss* (Fish)	10	NOEC	100	0.10	1.60E-07

Note: AF is assessment factor. AF=10 for long-term NOECs for three species for three trophic level organisms. AF=50 for two long-term NOECs for two trophic level organisms. AF=100 for one long-term NOEC for either fish or Daphnia (European Commission, 2003).

4. Conclusions

This study provides the first systematic investigation on the pollution status of NNIs in the farmland-river-marsh continuum in the largest marsh distribution area of China. The high residual concentrations and detection rates of NNIs suggest that the study area suffered from NNIs contamination. IMI, THM, and CLO were ubiquitous NNIs in soil, surface water, and sediments. In terms of spatial distributions, hydrological factors led to higher concentrations of NNIs in marsh surface water than Qixing River channel, while the buffering effect of marsh macrophytes led to an opposite distribution pattern of NNIs in sediments. Crop and land use types both affect NNIs distributions in soil, which showed the highest concentrations in soybean soil, followed by maize and rice soil, and higher concentrations in upland field than paddy field. The migration of NNIs from soils of different crops were influenced by not only precipitation amount, but also the application pattern of NNIs and planting area. The continued use of NNIs in agricultural lands may lead to their accumulation in soils, and migration to rivers and marshes through surface runoff, which could potentially increase the risks of NNIs to aquatic organisms. Due to the high water solubility of NNIs, fragile water environments are extremely vulnerable to NNIs pollution. Future monitoring plans should be estimated for measuring the major NNIs such as those presented in this study in sensitive ecosystems in order to help formulate future NNIs regulations.

Conflict of interest

The authors declare no conflict of interest.

Acknowledgments

This work was supported by the National Natural Science Foundation of China (No. 51779047).

References

Bass, C., Denholm, I., Williamson, M.S., Nauen, R., 2015. The global status of insect resistance to neonicotinoid insecticides. Pestic. Biochem. Physiol. 121, 78-87. https://doi.org/10.1016/j.pestbp.2015.04.004.

Bhutto, S.U., Xing, X.L., Shi, M.M., Mao, Y., Hu, T.P., Tian, Q., Cheng, C., Liu, W.J., Chen, Z.L., Qi, S.H., 2021. Occurrence and distribution of OCPs and PAHs in water, soil and sediment of Daye lake. J. Geochem. Explor. 226, 106769. https://doi.org/10.1016/j.gexplo.2021.106769.

Chen, Y.C., Zang, L., Shen, G.F., Liu, M.D., Du, W., Fei, J., Yang, L.Y., Chen, L., Wang, X.J., Liu, W.P., Zhao, M.R., 2019. Resolution of the ongoing challenge of estimating nonpoint source neonicotinoid pollution in the Yangtze River Basin using a modified mass balance approach. Environ. Sci. Technol. 53(5), 2539-2548. https://doi.org/10.1021/acs.est.8b06096.

Chen, D.W., Liu, Z.B., Barrett, H., Han, J.J., Lv, B., Li, Y., Li, J.G., Zhao, Y.F., Wu, Y.N., 2020. Nationwide Biomonitoring of Neonicotinoid Insecticides in Breast

Milk and Health Risk Assessment to Nursing Infants in the Chinese Population. J. Agric. Food. Chem. 68 (47), 13906-13915. https://doi.org/10.1021/acs.jafc.0c05769.

Cox-Foster, D.L., Conlan, S., Holmes, E.C., Palacios, G., Evans, J.D., Moran, N.A., Quan, P.L., Briese, T., Hornig, M., Geiser, D.M., Martinson, V., vanEngelsdorp, D., Kalkstein, A.L., Drysdale, A., Hui, J., Zhai, J.H., Cui, L.W., Hutchison, S.K., Simons, J.F., Egholm, M., Pettis, J.S., Lipkin, W.I., 2007. A metagenomic survey of microbes in honey bee colony collapse disorder. Science 318(5848), 283-287. https://doi.org/10.1126/science.1146498.

Cui, S., Yu, T., Zhang, F.X., Fu, Q., Hough, R., An, L.H., Gao, S., Zhang, Z.L., Hu, P., Zhu, Q.D., Pei, Z.X., 2020a. Understanding the risks from diffuse pollution on wetland eco-systems: The effectiveness of water quality classification schemes. Ecol. Eng. 155,105929. https://doi.org/10.1016/j.ecoleng.2020.105929.

Cui, S., Hough, R., Yates, K., Osprey, M., Kerr, C., Cooper, P., Coull, M., Zhang, Z.L., 2020b. Efects of season and sediment-water exchange processes on the partitioning of pesticides in the catchment environment: implications for pesticides monitoring. Sci. Total Environ. 698, 134228. https://doi.org/10.1016/j.scitotenv.2019.134228.

Cui, K., Wu, X.H., Wei, D.M., Zhang, Y., Cao, J.L., Xu, J., Dong, F.S., Liu, X.G., Zheng, Y.Q., 2021. Health risks to dietary neonicotinoids are low for Chinese residents based on an analysis of 13 daily-consumed foods. Environ. Int. 149, 106385.

https://doi.org/10.1016/j.envint.2021.106385.

European Commission, 2003. European Technical Guidance Document in Support of Commission Directive 93/67/EEC on Risk Assessment for new notified substances, Commission Regulation (EC) No. 1488/94 on Risk Assessment for existing substances, Directive 98/8/EC of the European Parliament and of the Council concerning the placing of biocidal products on the market. Part II. European Commission (EC) (ed).

Gibbons, D., Morrissey, C., Mineau, P., 2015. A review of the direct and indirect effects of neonicotinoids and fipronil on vertebrate wildlife. Environ. Sci. Pollut. Res. 22(1), 103-118. https://doi.org/10.1007/s11356-014-3180-5.

Goulson, D., 2013. An overview of the environmental risks posed by neonicotinoid insecticides. J. Appl. Ecol. 50, 977-987. https://doi.org/0.1111/1365-2664.12111.

Hallmann, C.A., Foppen, R.P.B., van Turnhout, C.A.M., de Kroon, H., Jongejans, E., 2014. Declines in insectivorous birds are associated with high neonicotinoid concentrations. Nature 511, 341-343. https://doi.org/10.1038/nature13531.

Han, W.C., Tian, Y., Shen, X.M., 2018. Human exposure to neonicotinoid insecticides and the evaluation of their potential toxicity: An overview. Chemosphere 192, 59-65. https://doi.org/10.1016/j.chemosphere.2017.10.149.

Hernando, M.D., Mezcua, M., Fernández-Alba, A.R., Barcelo, D., 2006. Environmental Risk Assessment of Pharmaceutical Residues in Wastewater Effluents, Surface Waters and Sediments. Talanta 69(2), 334-342.

https://doi.org/10.1016/j.talanta.2005.09.037.

Huang, Z.B., Li, H.Z., Wei, Y.L., Xiong, J.J., You, J., 2020. Distribution and ecological risk of neonicotinoid insecticides in sediment in South China: Impact of regional characteristics and chemical properties. Sci. Total Environ. 714, 136878. https://doi.org/10.1016/j.scitotenv.2020.136878.

Jeschke, P., Nauen, R., Schindler, M., Elbert, A., 2011. Overview of the Status and Global Strategy for Neonicotinoids. J. Agric. Food. Chem. 59(7), 2897-2908. https://doi.org/10.1021/jf101303g.

Ke, Y.X., Cui, S., FU, Q., Hough, R., Zhang, Z.L., Li, Y-F., 2022. Effects of pyrolysis temperature and aging treatment on the adsorption of Cd^{2+} and Zn^{2+} by coffee grounds biochar. Chemosphere 296, 134051. https://doi.org/10.1016/j.chemosphere.2022.134051.

Keddy P.A., 2010. Wetland Ecology: principles and conservation. New York: Cambridge University Press.

Li, K.Y., Cui, S., Zhang, F.X., Hough, R., Fu, Q., Zhang, Z.L., GAO, S., An, L.H., 2020. Concentrations, Possible Sources and Health Risk of Heavy Metals in Multi-Media Environment of the Songhua River, China. Int. J. Environ. Res. Public Health 17, 1766. https://doi.org/10.3390/ijerph17051766.

Liu, X., Wang, Y.B., Costanza, R., Kubiszewski, I., Xu, N., Gao, Z.A., Yuan, M.H., Geng, R.Y., Chen, H., Hu, X.K., 2019. Rice paddy fields' hidden value for typhoon protection in coastal areas. Ecol. Indic. 107, 105610.

https://doi.org/10.1016/j.ecolind.2019.105610.

Liu, Z.K., Cui, S., Zhang, L.M., Zhang, Z.L., Hough, R., Fu, Q., Li, Y.F., An, L.H., Huang, M.Z., Li, K.Y., Ke, Y.X., Zhang, F.X., 2021. Occurrence, variations, and risk assessment of neonicotinoid insecticides in Harbin section of the Songhua River, northeast China. Env. Sci. Ecotechnol. 8, 100128. https://doi.org/10.1016/j.ese.2021.100128.

Liu, Z.K., Zhang, L.M., Zhang, Z.L., An, L.H., Hough, R., Hu, P., Li, Y-F., Zhang, F.X., Wang, S., Zhao, Y.Q., Ke, Y.X., Cui, S., 2022. A review of spatiotemporal patterns of neonicotinoid insecticides in water, sediment, and soil across China. Environ. Sci. Pollut. Res. 29(37), 55336-55347. https://doi.org/10.1007/s11356-022-21226-6.

Lu, X.G., Liu, H.Y., Hu, J.M., 1996. Wetland resource protection and rational utilization in China. Chin. Geogr. Sci. 6(4), 313-320. https://doi.org/10.1007/s11769-996-0052-z.

Lu, X.G., Wang, R.F., 1996. Study on wetland biodiversity in China. Chin. Geogr. Sci. 6(1), 15-23. https://doi.org/10.1007/s11769-996-0032-3.

Mahai, G., Wan, Y.J., Xia, W., Yang, S.Y., He, Z.Y., Xu, S.Q., 2019. Neonicotinoid insecticides in surface water from the central Yangtze River, China. Chemosphere 229, 452-460. https://doi.org/10.1016/j.chemosphere.2019.05.040.

Mahai, G., Wan, Y.J., Xia, W., Wang, A.Z., Shi, L.S., Qian, X., He, Z.Y., Xu, S.Q., 2021. A nationwide study of occurrence and exposure assessment of neonicotinoid

insecticides and their metabolites in drinking water of China. Water Res. 189, 116630. https://doi.org/10.1016/j.watres.2020.116630.

Main, A.R., Fehr, J., Liber, K., Headley, J.V., Peru, K.M., Morrissey, C.A., 2017. Reduction of neonicotinoid insecticide residues in Prairie wetlands by common wetland plants. Sci. Total Environ. 579, 1193-1202. https://doi.org/10.1016/j.scitotenv.2016.11.102.

Morrissey, C.A., Mineau, P., Devries, J.H., Sanchez-Bayo, F., Liess, M., Cavallaro, M.C., Liber, K., 2015. Neonicotinoid contamination of global surface waters and associated risk to aquatic invertebrates: A review. Environ. Int. 74, 291-303. https://doi.org/10.1016/j.envint.2014.10.024.

Naumann, T., Bento, C. P.M., Wittmann, A., Gandrass, J., Tang, J.H., Zhen, X.M., Liu, L., Ebinghaus, R., 2022. Occurrence and ecological risk assessment of neonicotinoids and related insecticides in the Bohai Sea and its surrounding rivers, China. Water Res. 209, 117912. https://doi.org/10.1016/j.watres.2021.117912.

Niu, Y.H., Wang, L., Wang, Z., Yu, S.X., Zheng, J.Y., Shi, Z.H., 2022. High-frequency monitoring of neonicotinoids dynamics in soil-water systems during hydrological processes. Environ. Pollut. 292(Part A), 118219. https://doi.org/10.1016/j.envpol.2021.118219.

Pan, Y.F., Liu, S., Tian, F., Chen, H.G., Xu, X.R., 2022. Tetrabromobisphenol A and hexabromocyclododecanes in sediments from fishing ports along the coast of South China: Occurrence, distribution and ecological risk. Chemosphere, 302,

134872. https://doi.org/10.1016/j.chemosphere.2022.134872.

Tang, T.G., Cheng, Z.N., Xu, B.Q., Zhang, B.L., Zhu, S.Y., Cheng, H.R., Li, J., Chen, Y.J., Zhang, G., 2020. Triple Isotopes ($\delta^{13}C$, $\delta^{2}H$, and $\Delta^{14}C$) Compositions and Source Apportionment of Atmospheric Naphthalene: A Key Surrogate of Intermediate-Volatility Organic Compounds (IVOCs). Environ. Sci. Technol. 54(9), 5409-5418. https://pubs.acs.org/doi/10.1021/acs.est.0c00075.

Van Dijk, T.C., Van Staalduinen, M.A., Van der Sluijs, J.P., 2013. Macro-invertebrate declinein surface water polluted with imidacloprid. PLoS One 8(5), e62374. https://doi.org/10.1371/journal.pone.0062374.

Wan, Y.J., Wang, Y., Xia, W., He, Z.Y., Xu, S.Q., 2019. Neonicotinoids in raw, finished, and tap water from Wuhan, Central China: Assessment of human exposure potential. Sci. Total Environ. 675, 513-519. https://doi.org/10.1016/j.scitotenv.2019.04.267.

Wang, R.Y., Yuan, Y.P., Yen, H., Grieneisen, M., Arnold, J., Wang, D., Wang, C.Z., Zhang, M.H., 2019. A review of pesticide fate and transport simulation at watershed level using SWAT: Current status and research concerns. Sci. Total Environ. 669, 512-526. https://doi.org/10.1016/j.scitotenv.2019.03.141.

Xiong, J.J., Wang, Z., Ma, X., Li, H.Z., You, J., 2019. Occurrence and risk of neonicotinoid insecticides in surface water in a rapidly developing region: Application of polar organic chemical integrative samplers. Sci. Total Environ. 648, 1305-1312. https://doi.org/10.1016/j.scitotenv.2018.08.256.

Zhang, C., Dionysiou, D.D., Wen, R.B., Zhang, H.K., Wan, X., Wang, X.Z., Li, F., Li, Y.Q., Zhou, Q., Ying, G.G., Huang, M.Z., 2022. Inference of emission history of neonicotinoid pesticides from marine sediment cores impacted by riverine runoff of a developed agricultural region: The Pearl River Basin, China. Water Res. 218, 118475. https://doi.org/10.1016/j.watres.2022.118475.

Zhang, F.X., Cui, S., Gao, S., Hough, R., Hu, P., Zhang, Z.L., Fu, Q., Yu, T., Li, K.Y., 2020. Heavy metals exposure risk to Eurasian Spoonbill (*Platalea leucorodia*) in wetland ecosystem, Northeast China. Ecol. Eng. 157, 105993. https://doi.org/10.1016/j.ecoleng.2020.105993.

Zhang, F.X., Meng, B., Gao, S., Hough, R., Hu, P., Zhang, Z.L., Yu, S.P., Li, K.Y., Liu, Z.K., Cui, S., 2021. Levels, Inventory, and Risk Assessment of Heavy Metals in Wetland Ecosystem, Northeast China: Implications for Snow Cover Monitoring. Water 13(16), 2161. https://doi.org/10.3390/w13162161.

Zhang, Y.Q., Lu, Y.L., Wang, P., Li, Q.F., Zhang, M., Johnson, A.C., 2018. Transport of Hexabromocyclododecane (HBCD) into the soil, water and sediment from a large producer in China. Sci. Total Environ. 610, 94-110. https://doi.org/10.1016/j.scitotenv.2017.08.039.

Zhou, Y.T., Wu, J.X., Wang, B., Duan, L., Zhang, Y.Z., Zhao, W.X., Wang, F., Sui, Q., Chen, Z.Y., Xu, D.J., Li, Q.X., Yu, G., 2020. Occurrence, source and ecotoxicological risk assessment of pesticides in surface water of Wujin District (northwest of Taihu Lake), China. Environ. Pollut. 265(Part A), 114953.

https://doi.org/10.1016/j.envpol.2020.114953.

Supporting Information

Diffusion pollution of neonicotinoid insecticides in wetland ecosystem: Has the cultivation of different crops become the major sources?

Zhikun Liu[a,b], Song Cui [a,b*], Qiang Fu[a,b], Fuxiang Zhang[a,b], Zulin Zhang[c], Rupert Hough[c], Lihui An[d], Yi-Fan Li [a,b], Leiming Zhang[e*]

[a] *International Joint Research Center for Persistent Toxic Substances (IJRC-PTS), School of Water Conservancy and Civil Engineering, Northeast Agricultural University, Harbin, Heilongjiang 150030, China*

[b] *Research Center for Eco-Environment Protection of Songhua River Basin, Northeast Agricultural University, Harbin, Heilongjiang 150030, China*

[c] *The James Hutton Institute, Craigiebuckler, Aberdeen, AB15 8QH, UK*

[d] *State Environmental Protection Key Laboratory of Estuarine and Coastal Research, Chinese Research Academy of Environmental Sciences, Beijing 100012, China*

[e] *Air Quality Research Division, Science and Technology Branch, Environment and Climate Change Canada, Toronto, Ontario M3H 5T4 Canada*

5 TEXTS

9 TABLES

5 FIGURES

Text S1 Chemicals and reagents

The analytical standards of the eight NNIs, including imidacloprid (IMI, purity 99.8%), thiamethoxam (THM, 99.2%), acetamiprid (ACE, 99.8%), dinotefuran (DIN, 99.8%), thiacloprid (THA, 99.3%), nitenpyram (NTP, 98.6%), imidaclothiz (IMIT, 99.2%), and clothianidin (CLO, 99.8%), were purchased from Alta Scientific Co., Ltd. (Tianjin, China). The isotope-labeled internal standards, including imidacloprid-d_4 (IMI-d_4, 99.5%) and thiamethoxam-d_3 (THM-d_3, 99.5%), were obtained from CDN Isotopes (Quebec, Canada), and clothianidin-d_3 (CLO-d_3, > 98.5%) was from Dr. Ehrenstrofer (Augsburg, Germany). All standard solutions were stored at -20℃. Acetonitrile and methanol (HPLC-MS grade) were purchased from Fisher Chemical, Inc. (Waltham, MA, USA), and the primary secondary amine (PSA) was obtained from Agela Technologies (Tianjin, China).

Text S2 Sample pretreatment

The target NNIs in water samples were extracted using the previously described method (Liu et al., 2021; Mahai et al., 2019). Briefly, water samples (each in 1 L) were filtered through a Teflon filter and spiked with an internal standards mixture (50 μL of 1 mg/L) before being processed using Waters Oasis HLB solid-phase extraction (SPE) cartridges (500 mg, 6 cc, Milford, MA, USA). The cartridge was preconditioned with 5 mL methanol and 5 mL ultra-pure water in sequence. After being loaded on the water samples, the target compounds were eluted with 5 mL ultra-pure water, followed by 5 mL methanol. The eluents were evaporated at 35℃ under a gentle nitrogen stream until

nearly dry, then redissolved in 1 mL of 25% acetonitrile in water and passed through a 0.22 μm filter for analysis.

The sediment and soil were pretreated using the dispersive solid-phase extraction procedure (Liu et al., 2021; Zhou et al., 2018; Dankyi et al., 2014). In detail, a 5 g freeze-dried sample was transferred into a PTFE centrifuge tube, spiked with 50 μL mixed internal standard (1 mg/L), and left to stand for 45 min. After adding 5 mL of ultrapure water and 10 mL of acetonitrile, the tube was shaken for 1 min and vortexed for 1 min. A 4 g $MgSO_4$ and 1 g NaCl were added into the tube, followed by vortexing for 1 min. Then the tube was centrifuged at 5000 rpm for 5 min. A 6 mL supernatant was separated into a clean PTFE tube containing 200 mg primary secondary amine (PSA). The extract was vortexed for 2 min and centrifuged at 5000 rpm for 5 min. An aliquot (5 mL) of the upper organic solution was evaporated to near dryness by a gentle nitrogen stream at 35℃ and reconstituted in 1 mL of 25% acetonitrile in water. The extract was filtrated through a 0.22 μm PTFE membrane for HPLC-MS/MS analysis.

Text S3 Instrumental analysis

The chemical analysis was carried out on AB SCIEX Triple Quad 5500 HPLC-MS/MS (Framingham, MA, USA) using an electrospray ionization source in the positive ion mode (ESI^+) with multiple reactions monitoring (MRM) mode. The injection volume was 2 μL. The analytes were separated at 25°C using a Phenomenex Kinetex® C18 column (100 mm × 2.1 mm, 1.7 μm). The mobile phase was 0.1% formic acid-water

solution (A) and acetonitrile (B), and the flow rate of the mobile phase was set at 0.3 mL/min. A gradient program of the mobile phase began with 95% A and 5% B, followed by a linear decrease from 95% to 65% A in 3 min, then to 45% A in 6 min, and finally reverted to 95% in 9 min before ending the program in 12 min. In the MS/MS analysis, nitrogen was used as atomizing gas. The pressure of curtain and collision gas was set at 35 and 7 psi, respectively. Ion spray voltage was set at 5500 V. The temperature of drying gas was set at 550 °C. The pressure of ion source gas1 and gas2 was set at 55 and 60 psi, respectively. Collision cell exit potential and entrance potential were 16.0 and 10.0 V, respectively.

Text S4 Surface runoff

Pesticides can migrate in soil water or adsorb on soil particles, depending on the adsorption coefficient (K_p) of pesticides in soil **(**Eq. (1)) (Wang et al., 2019):

$$K_p = \frac{C_{solidphase}}{C_{solution}} = K_{oc} \cdot \frac{orgC}{100} \quad (1)$$

where $C_{solidphase}$ (mg/kg) and $C_{solution}$ (mg/L) are the concentrations of pesticide within soil solid and liquid phases, respectively; K_{oc} is the soil adsorption coefficient normalized for the soil organic carbon content (m^3/ton); and *orgC* is the concent of organic carbon in the soil.

The overall degradation of pesticide in the soil environment can be calculated by half-life time (DT_{50}) using Eq. (2):

$$pst_{s,ly,t} = pst_{s,ly,0} \cdot \exp(\frac{0.693}{hlife} \cdot t) \quad (2)$$

Where $pst_{s,ly,t}$ and $pst_{s,ly,0}$ are the amounts of pesticide in the soil layer at times t and 0

(kg/ha), respectively; and, *hlife* is the half-life time of the pesticide in the soil (d). We assumed that 90% of the sprayed IMI enters the soil and that the uptake of IMI by maize after the seed treatment is approximately 20% (Li et al., 2018; Sur and Stork, 2003). The amount of pesticide in the soil soluble phase that is ready for transport is calculated using Eq. (3):

$$pst_{flow} = pst_{s,ly,t}\left(1 - \exp\left[\frac{-w_{mobile}}{SAT_{ly} + K_p \cdot \rho_b \cdot depth_{ly}}\right]\right) \quad (3)$$

where pst_{flow} is the amount of pesticide contained in the soil water flux (kg/ha); w_{mobile} is the amount of mobile water (mm); SAT_{ly} is the amount of water in the soil layer at saturation (mm); ρ_b is the bulk density of the soil layer (g/cm^3); and $depth_{ly}$ is the depth of the soil layer (mm). The amount of soluble pesticide transported by surface runoff is calculated using Eq. (4):

$$pst_{surf} = \beta_{pst}\frac{pst_{flow}}{w_{mobile}}\alpha P_i \quad (4)$$

where pst_{surf} is the mass of pesticide transported by surface runoff from soil on per hectare basis (kg/ha); β_{pst} is the pesticide percolation coefficient; α is the surface runoff coefficient; and P_i is precipitation amount from the time of IMI application to the time of sample collection (mm).

Text S5 Calculation of PNEC

$$PNEC = L(E)C_{50} \text{ or } NOEC/AF \quad (5)$$

where NOEC is the lowest no observed effective concentration; EC_{50} and LC_{50} are the median effective concentration and the median lethal concentration, respectively; and AF is the assessment factor. NOEC and $L(E)C_{50}$ of NNIs were obtained from the Pesticide Properties Database (PPDB) (Table S5).

Table S1 Sampling sites of soil, surface water, and sediment from the farmland-river-marsh continuum.

Sampling site	Longitude	Latitude	Crop types	Sampling site	Longitude	Latitude
T1	131°44′19″	46°32′17″	maize	S1	131°41′48″	46°33′42″
T2	131°48′27″	46°34′56″	maize	S2	131°48′18″	46°36′29″
T3	131°49′58″	46°37′39″	maize	S3	131°55′11″	46°38′44″
T4	131°52′38″	46°40′13″	rice	S4	132°1′17″	46°42′08″
T5	131°52′20″	46°34′49″	maize	S5	132°2′33″	46°41′49″
T6	131°56′16″	46°34′45″	maize	S6	132°6′07″	46°42′16″
T7	131°56′18″	46°37′26″	soybean	S7	132°7′08″	46°43′06″
T8	131°56′37″	46°42′52″	rice	S8	132°8′10″	46°42′54″
T9	131°59′30″	46°45′30″	rice	S9	132°9′28″	46°42′16″
T10	132°0′23″	46°40′01″	soybean	S10	132°10′55″	46°42′24″
T11	132°0′16″	46°37′21″	rice	S11	132°11′33″	46°42′52″

T12	132°4′22″	46°39′56″	soybean	S12	132°10′12″	46°43′31″
T13	132°4′41″	46°45′20″	rice	S13	132°9′11″	46°43′28″
T14	132°4′43″	46°47′59″	rice	S14	132°9′14″	46°45′12″
T15	132°8′39″	46°47′55″	rice	S15	132°10′47″	46°47′00″
T16	132°7′37″	46°40′12″	soybean	S16	132°12′26″	46°48′22″
T17	132°11′29″	46°37′11″	rice	S17	132°17′25″	46°43′42″
T18	132°11′45″	46°39′52″	rice	S18	132°17′16″	46°43′26″
T19	132°15′44″	46°41′13″	rice	S19	132°24′09″	46°43′18″
T20	132°20′06″	46°41′09″	rice	S20	132°23′51″	46°43′00″
T21	132°23′24″	46°42′00″	maize			
T22	132°28′22″	46°47′23″	soybean			

Note: T means soil sampling sites; S means water and sediment sampling sites

Table S2 Physicochemical properties of neonicotinoid insecticides.

Neonicotinoids	Molecular formula	Molecular weight	Water solubility (20℃, pH=7) /(mg/L)	Vapor pressure (20℃) /(mPa)	Water-sediment DT_{50}/(d)	Soil degradation (typical) DT_{50}/(d)	Water photolysis DT_{50}/(d)	log K_{oc} [a]	log K_{ow} [b]	GUS
Imidacloprid	$C_9H_{10}ClN_5O_2$	255.70	610	4×10^{-7}	129	191	<1	2.19~2.90	0.57	4.33
Thiamethoxam	$C_8H_{10}ClN_5O_3S$	291.72	4,100	6.6×10^{-6}	40	50	2.7~39.5	1.75	-0.13	3.82
Dinotefuran	$C_7H_{14}N_4O_3$	202.21	39,830	1.7×10^{-3}	NA	82	<2	1.41	-0.55	4.31
Acetamiprid	$C_{10}H_{11}ClN_4$	222.67	2,950	1.73×10^{-4}	NA	1.6	34	2.30	0.80	0.35
Thiacloprid	$C_{10}H_9ClN_4S$	252.72	184	3.0×10^{-7}	14.8	0.88	10~63	3.67	1.26	-0.02
Clothianidin	$C_6H_8ClN_5O_2S$	249.68	340	2.8×10^{-8}	56.4	545	<1	2.08	0.91	5.25
Nitenpyram	$C_{11}H_{15}ClN_4O_2$	270.71	590,000	1.1×10^{-3}	NA	8	NA	1.78	-0.66	2.00
Imidaclothiz	$C_7H_8ClN_5O_2S$	261.69	5,000 [c]	NA[d]	40	3.1	NA	0.93[e]	NA	1.51

Data source: Pesticide Products Database (PPDB), University of Hertfordshire, available at http://sitem.herts.ac.uk/aeru/ppdb/index.htm and the Hazardous Substances Data Bank (HSDB), available at http://toxnet.nlm.nih.gov/cgi-bin/sis/htmlgen?HSDB

[a] K_{oc}: organic carbon-water partition coefficient

[b] K_{ow}: octanol-water partition coefficient

[c] 25℃

[d] NA: not available

Table S3 Related information of individual neonicotinoid insecticides for HPLC-MS/MS analysis.

Compound	Precursor ions (m/z)	Product ions (m/z)	t_R (min)	Regression equation	Linearity	Recovery (%)		MDL	
						Water	Sediment and soil	Water (ng/L)	Sediment and soil (ng/g)
Imidacloprid	256.1	175.0	3.61	Y=21873X+12861	0.999	92.1±3.3	95.2±6.5	0.01	0.03
Clothianidin	250.0	169.1	3.45	Y=17265X+2605	0.999	86.3±4.2	79.8±4.3	0.02	0.06
Thiamethoxam	292.2	211.0	3.08	Y=30714X+47702	0.997	88.3±4.1	96.2±6.8	0.01	0.03
Dinotefuran	203.1	114.1	2.13	Y=14625X+8106	0.999	98.5±2.5	85.6±3.9	0.10	0.30
Nitenpyram	271.2	126.1	2.64	Y=9637X+2414	0.999	108.9±6.6	84.6±5.3	0.05	0.15
Thiacloprid	253.1	126.1	4.29	Y=125143X+33171	0.999	95.3±3.1	89.3±5.2	0.01	0.03
Acetamiprid	223.0	126.0	3.85	Y=82214X+18452	0.999	91.4±3.6	106.5±6.8	0.01	0.03
Imidaclothiz	261.9	181.0	3.74	Y=26010X+1470	0.999	89.5±4.6	92.4±4.5	0.01	0.03

$t_{R:}$ retention time; MDL: method detection limit.

Table S4 Toxicity data of NNIs to the sensitive aquatic species.

Compound	Species	trophic levels	Effective concentration (mg/L)	Endpoint	AF
IMI	*Oncorhynchus mykiss*	Fish	9.02	NOEC	
	Daphnia magna	Daphnia	1.8	NOEC	10
	Scenedesmus subspicatus	Algae	10	NOEC	
THM	*Oncorhynchus mykiss*	Fish	20	NOEC	
	Daphnia magna	Daphnia	100	NOEC	50
	Pseudokirchneriella subcapitata	Algae	100	EC50	
CLO	*Pimephales promelas*	Fish	20	NOEC	
	Daphnia magna	Daphnia	0.12	NOEC	50
	Pseudokirchneriella subcapitata	Algae	55	EC_{50}	
ACE	*Pimephales promelas*	Fish	19.2	NOEC	
	Daphnia magna	Daphnia	5	NOEC	50
	Scenedemus subspicatus	Algae	98.3	EC_{50}	
NTP	*Oncorhynchus mykiss*	Fish	10	NOEC	
	Daphnia magna	Daphnia	10,000	EC_{50}	100
	Pseudokirchneriella subcapitata	Algae	26	EC_{50}	

NOEC and L(E)C_{50} of NNIs were obtained from the Pesticide Properties Database (PPDB), available at http://sitem.herts.ac.uk/aeru/ppdb/index.htm. According to the Technical Guidance Document (European Commission, 2003) evaluation factors are selected based on biological toxicity data. The acute toxicity data AF is 1,000; when the chronic toxicity data meets three trophic levels, AF is 10; when two trophic levels are satisfied, AF is selected 50; when a trophic level is met, AF is taken as 100.

Table S5 Concentrations of NNIs in soil (ng/g, dw) from the farmland-river-marsh continuum.

Sampling site	IMI	THM	THA	IMIT	NTP	DIN	CLO	ACE	TOC (%)
T1	25.2	0.52	ND	0.01	ND	ND	0.68	ND	3.99
T2	2.26	1.28	ND	ND	ND	ND	0.25	ND	4.22
T3	1.45	0.55	ND	ND	ND	ND	0.24	ND	4.35
T4	2.02	1.18	ND	ND	ND	ND	0.26	ND	3.62
T5	1.55	29.3	ND	ND	ND	ND	14.8	ND	3.11
T6	69.7	4.73	ND	ND	ND	ND	7.70	ND	4.70
T7	7.60	4.54	ND	ND	ND	ND	1.76	ND	3.99
T8	1.28	0.77	ND	ND	ND	ND	0.08	ND	3.49
T9	10.7	1.48	ND	ND	ND	ND	0.34	ND	3.83
T10	51.3	1.00	ND	ND	ND	ND	0.59	ND	6.70
T11	3.33	8.24	ND	ND	ND	ND	0.38	ND	4.88
T12	17.0	3.86	ND	ND	ND	ND	1.55	ND	6.83
T13	3.05	1.46	ND	ND	ND	ND	0.08	ND	4.98
T14	3.53	0.96	ND	ND	ND	ND	0.15	ND	4.76
T15	121	6.72	ND	ND	ND	ND	3.30	ND	4.89
T16	122	6.89	ND	ND	ND	ND	2.95	ND	6.89
T17	5.13	1.31	ND	ND	ND	ND	0.51	ND	6.33
T18	6.47	2.08	ND	ND	ND	ND	0.88	ND	6.60
T19	11.6	0.89	ND	ND	ND	ND	0.34	0.08	4.46
T20	2.98	0.56	ND	ND	ND	ND	0.09	ND	3.49
T21	39.4	0.80	ND	ND	ND	ND	2.11	ND	3.89
T22	133	1.20	ND	ND	ND	ND	2.37	ND	3.74

Table S6 Concentrations of NNIs in water (ng/L) from the farmland-river-marsh continuum.

Sampling site	IMI	THM	THA	IMIT	NTP	DIN	CLO	ACE
S1	6.09	4.17	ND	ND	ND	ND	0.70	ND
S2	13.3	10.2	ND	ND	ND	ND	1.18	0.28
S3	8.80	6.48	ND	ND	ND	ND	0.96	0.12
S4	11.0	11.7	ND	ND	ND	ND	0.85	0.19
S5	10.3	8.86	ND	ND	ND	ND	1.24	ND
S6	7.97	8.30	ND	ND	ND	ND	1.64	ND
S7	11.5	10.2	ND	ND	ND	ND	1.24	0.16
S8	10.1	6.51	ND	ND	ND	ND	0.97	ND
S9	25.6	24.3	ND	ND	ND	ND	1.82	ND
S10	7.27	6.86	ND	ND	ND	ND	1.29	ND
S11	7.40	6.06	ND	ND	ND	ND	1.10	ND
S12	6.91	6.65	ND	ND	ND	ND	0.97	ND
S13	6.73	5.20	ND	ND	ND	ND	1.15	ND
S14	12.9	4.05	ND	ND	0.19	ND	0.81	ND
S15	7.78	5.07	ND	ND	0.13	ND	0.96	ND
S16	12.0	12.9	ND	ND	ND	ND	1.39	ND
S17	12.6	22.9	ND	ND	ND	ND	2.39	ND
S18	10.5	23.8	ND	ND	ND	ND	2.47	ND
S19	6.85	15.4	ND	ND	ND	ND	1.72	ND
S20	2.84	ND	ND	ND	ND	ND	0.36	ND

Table S7 Concentrations of NNIs in sediment (ng/g, dw) from the farmland-river-marsh continuum.

Sampling site	IMI	THM	THA	IMIT	NTP	DIN	CLO	ACE	TOC (%)
S1	3.85	1.27	ND	ND	ND	ND	0.47	0.19	8.26
S2	0.98	0.54	ND	ND	ND	ND	0.08	ND	5.01
S3	3.40	1.42	ND	ND	ND	ND	0.41	ND	4.31
S4	4.37	1.84	ND	ND	ND	ND	0.73	0.01	3.98
S5	2.52	1.48	ND	ND	ND	ND	0.22	ND	4.08
S6	1.53	0.49	ND	ND	ND	ND	0.14	ND	2.81
S7	4.79	1.53	ND	ND	ND	ND	0.70	0.06	4.32
S8	1.83	2.85	ND	ND	ND	ND	0.15	ND	3.93
S9	2.18	1.39	ND	ND	ND	ND	0.13	ND	3.40
S10	0.89	0.56	ND	ND	ND	ND	0.09	ND	1.81
S11	1.95	0.60	ND	ND	ND	ND	0.08	ND	3.10
S12	1.92	0.59	ND	ND	ND	ND	0.13	ND	2.27
S13	0.89	0.60	ND	ND	ND	ND	0.32	ND	2.48
S14	0.80	1.06	ND	ND	ND	ND	0.36	ND	3.83
S15	1.19	1.41	ND	ND	ND	ND	0.31	ND	3.64
S16	1.04	0.72	ND	ND	ND	ND	0.16	ND	2.75
S17	0.57	1.87	ND	ND	ND	ND	0.12	ND	5.28
S18	1.10	0.96	ND	ND	ND	ND	0.14	ND	3.98
S19	6.36	1.92	ND	ND	ND	ND	0.13	ND	3.74
S20	0.81	1.81	ND	ND	ND	ND	0.12	ND	3.70

Table S8 IMI is used for agricultural production scenarios in the study area.

crop types	date of application	usage pattern	Maximum usage	Number of days[b]
rice	June 15th	*spray*	63 g/ha	132
maize	May 5th	*seed coating*	183.7 g/ha[a]	173
soybean	June 15th	*spray*	10.8 g/ha	132

[a] The usage of IMI on maize is mainly by seed coating (490 g IMI for 100 kg maize seeds), and the maximum use amount of IMI is calculated by the use of maize seeds per hectare (37.5 kg maize seeds).

[b] The number of days from the date of IMI application to the last rainfall before sample collection (8th October).

Table S9 Input parameters to characterize the pst_{surf} values.

Parameters	Value	Parameters	Value
β_{pst}	0.8	$depth_{ly}$	10 mm
P_i [a]	685.8 mm (paddy fields) 876.3 mm (maize fields) 685.8 mm (soybean fields)	*cultivated area*	40,816 ha (paddy fields) 71,820 ha (maize fields) 44,460 ha (soybean fields)
α	34.70% (paddy fields) 49.69% (upland fields)	SAT_{ly}	2 mm
w_{mobile}	1 mm	*orgC*	4.71%
ρ_b	2.65 g/cm^3		

Parameters are derived from default values, measured values, or statistical data.

[a] Precipitation amount is the sum of rainfall from the date of IMI application to the last rainfall before sample collection (8th October).

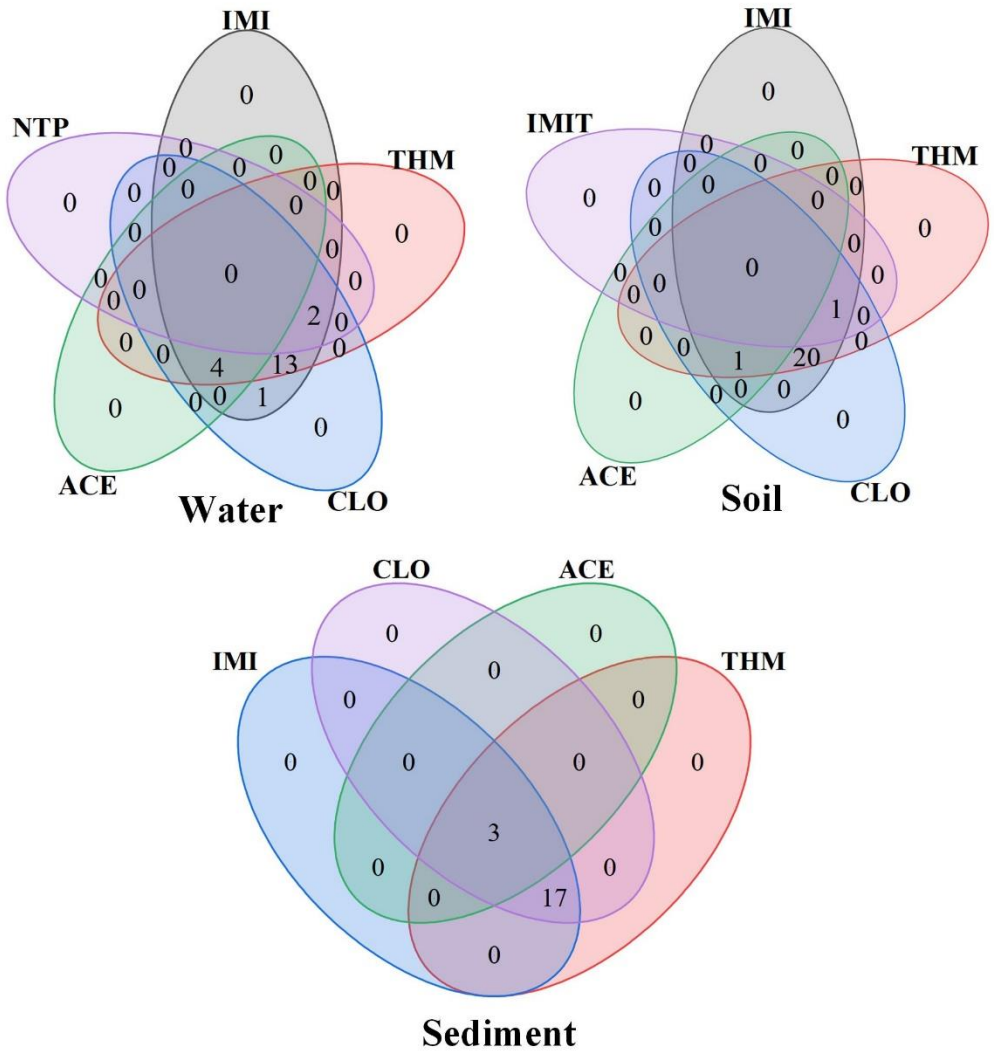

Fig. S1 Venn diagram of NNIs detected in water, soil and sediment samples collected from the farmland-river-swamp continuum.

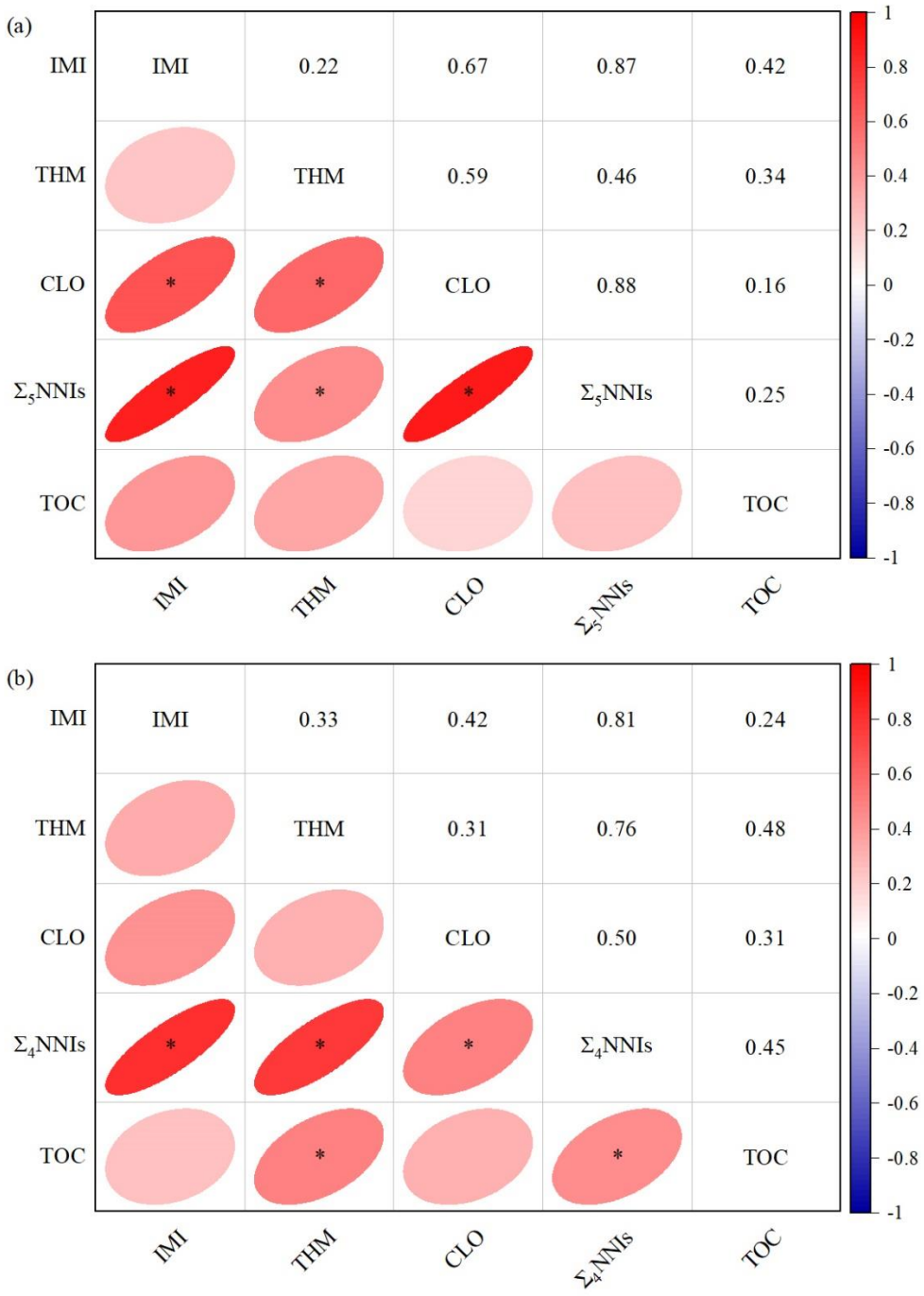

Fig. S2 Spearman correlation coefficients between TOC and NNIs in (a) soil and (b) sediment.

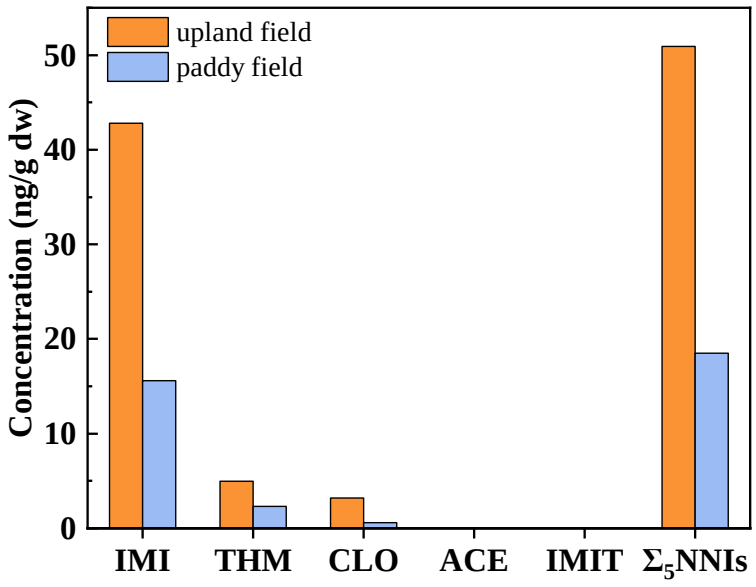

Fig. S3 The concentrations of NNIs in different type of land use soils. NNIs for upland fields were calculated as the mean of the concentrations in maize- and soybean-growing soils, while NNIs for paddy fields were the mean of the concentrations in the rice-growing soils.

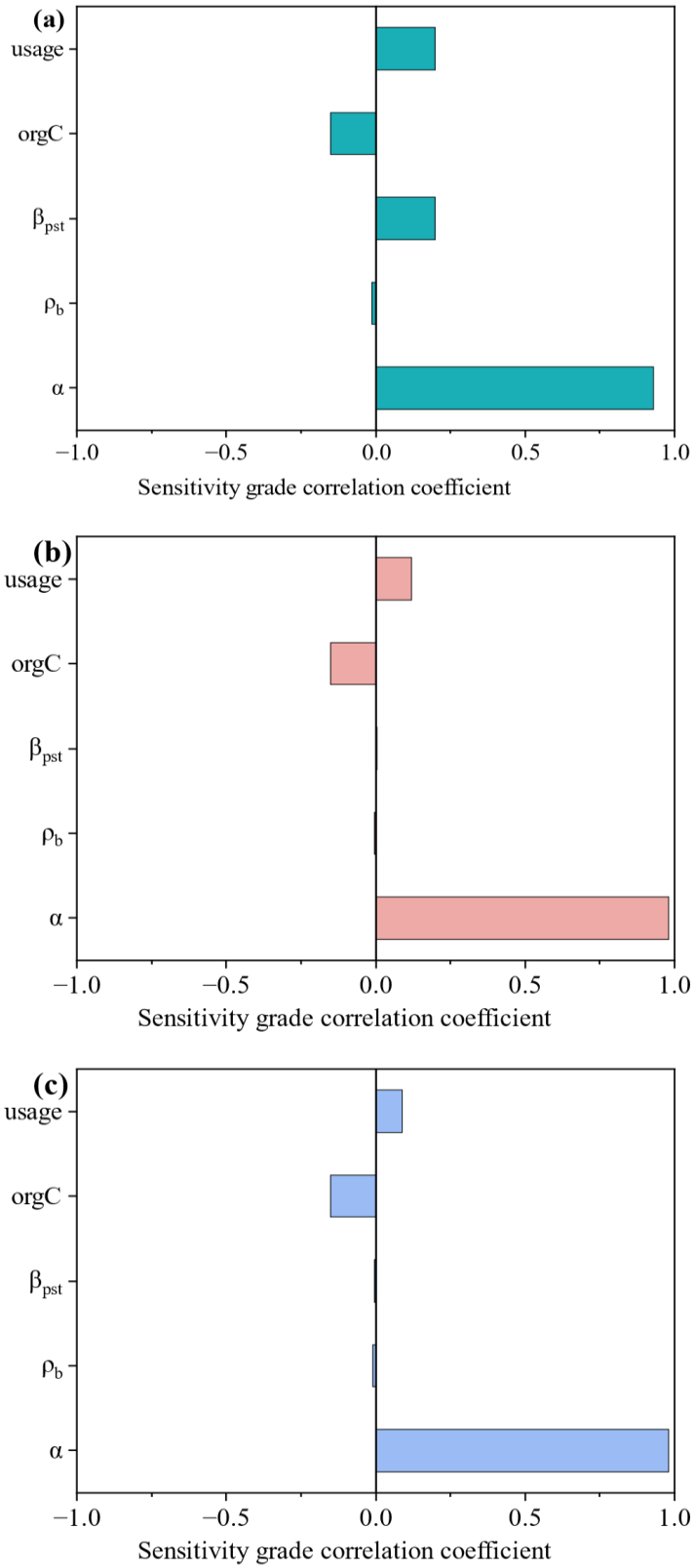

Fig. S4 Sensitivity of calculated parameters of migration flux by surface runoff. (a) paddy fields; (b) maize files; (c) soybean fields

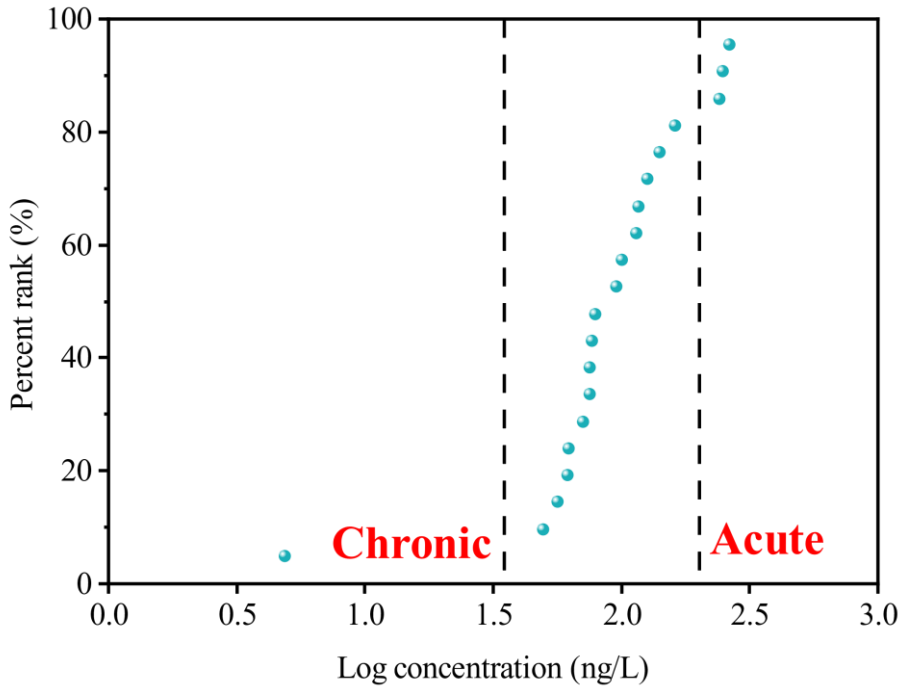

Fig. S5 Environmental exposure distributions of NNIs in surface water.

References

European Commission, 2003. European Technical Guidance Document in Support of Comission Directive 93/67/EEC on Risk Assessment for new notified substances, Commission Regulation (EC) No. 1488/94 on Risk Assessment for existing substances, Directive 98/8/EC of the European Parliament and of the Council concerning the placing of biocidal products on the market. Part II. European Commission (EC) (ed).

Dankyi, E., Gordon, C., Carboo, D., Fomsgaard, I.S., 2014. Quantification of neonicotinoid insecticide residues in soils from cocoa plantations using a QuEChERs extraction procedure and LC-MS/MS. Sci. Total Environ. 499, 276-

283.

Li, T.T., Zheng, S.S., Wang, J., Zhao, Y.H., Li, C., 2018. A review on occurrence and transformation behaviors of neonicotinoid pesticides. Asian Journal of Ecotoxicology 13(4), 9-21. (in Chinese)

Liu, Z.K., Cui, S., Zhang, L.M., Zhang, Z.L., Hough, R., Fu, Q., Li, Y.F., An, L.H., Huang, M.Z., Li, K.Y., Ke, Y.X., Zhang, F.X., 2021. Occurrence, variations, and risk assessment of neonicotinoid insecticides in Harbin section of the Songhua River, northeast China. Environmental Science and Ecotechnology 8, 100128.

Mahai, G., Wan, Y.J., Xia, W., Yang, S.Y., He, Z.Y., Xu, S.Q., 2019. Neonicotinoid insecticides in surface water from the central Yangtze River, China. Chemosphere 229, 452-460.

Sur, R., Stork, A., 2003. Uptake, translocation and metabolism of imidacloprid in plants. Bull. Insectology 56, 35-40.

Wang, R.Y., Yuan, Y.P., Yen, H., Grieneisen, M., Arnold, J., Wang, D., Wang, C.Z., Zhang, M.H., 2019. A review of pesticide fate and transport simulation at watershed level using SWAT: Current status and research concerns. Sci. Total Environ. 669, 512-526.

Zhou, Y., Lu, X.X., Fu, X.F., Yu, B., Wang, D., Zhao, C., Zhang, Q., Tan, Y., Wang, X.Y., 2018. Development of a fast and sensitive method for measuring multiple neonicotinoid insecticide residues in soil and the application in parks and residential areas. Analytica Chimica Acta, 1016, 19-28.